

Ab Initio Structures and Vibrational Spectra of  $\text{Li}[\text{C}(\text{CF}_3\text{SO}_2)_3]$  and  $\text{Li}[\text{CH}(\text{CF}_3\text{SO}_2)_2]$ Patrik Johansson<sup>†</sup>

Department of Experimental Physics, Chalmers University of Technology, SE-412 96 Göteborg, Sweden

Received: May 10, 2001; In Final Form: June 15, 2001

The structures and vibrational spectra for the anions  $[\text{C}(\text{CF}_3\text{SO}_2)_3]^-$  and  $[\text{CH}(\text{CF}_3\text{SO}_2)_2]^-$  as well as their ion pairs with lithium have been calculated. Ab initio self-consistent field molecular orbital Hartree–Fock and density functional theory calculations, using the hybrid B3LYP functional, have been performed, both using the 6-31G\* basis set. The results are compared with earlier calculational work on the more commonly used TFSI anion,  $[\text{N}(\text{CF}_3\text{SO}_2)_2]^-$ , and with experimental IR spectra. The localization of the single negative charge toward the  $\text{SO}_2$  groups is slightly less pronounced in the  $[\text{C}(\text{CF}_3\text{SO}_2)_3]^-$  anion, which results in a lower lithium ion affinity. Also, the double bond character for the central  $\text{Sx}-\text{C1}$  bonds is smaller compared to that of  $[\text{CH}(\text{CF}_3\text{SO}_2)_2]^-$ . The two anions' advantages/disadvantages as polymer electrolyte components are discussed.

## Introduction

The lithium salts used in solid polymer electrolytes (SPEs) (a mix of a polymer and an inorganic salt) preferably have large monocharged anions with a strongly delocalized charge to be able to provide a large number of charge carriers in the polymer matrix. Therefore, well-known leaving groups such as the triflate anion ( $\text{CF}_3\text{SO}_3^-$ ) and its lithium salt were initially used, together with more traditional anions such as  $\text{ClO}_4^-$  and  $\text{PF}_6^-$ . More recently other anions based on the strong electron-withdrawing power of the  $\text{CF}_3\text{SO}_2^-$  moiety have been employed, the TFSI anion,  $[\text{N}(\text{CF}_3\text{SO}_2)_2]^-$ , being the most used and well-known.

Ab initio modeling has been an important tool to evaluate different anions' potential for usage in SPEs. For example, a potential energy surface for the TFSI anion was obtained by ab initio calculations and showed the so-called "plasticizing effect" of this anion to probably be due to its internal flexibility with low energy barriers between two stable conformations.<sup>1</sup> Similar studies have recently been performed on both the PFSI,  $[\text{N}(\text{C}_2\text{F}_5\text{SO}_2)_2]^-$ , and the  $[\text{N}(\text{CF}_3\text{SO}_2)(\text{CF}_3(\text{CF}_2)_3\text{SO}_2)_2]^-$  anions.<sup>2,3</sup> Such studies are the basis for predictional calculations of the anions' lithium ion affinities and also provide important structural/dynamical information that in many cases is inaccessible by other methods.

Using knowledge obtained from earlier studies,<sup>1,2,4</sup> we here study two anions based on a central carbon atom and the  $\text{CF}_3\text{SO}_2^-$  moiety: TriTFSM,  $[\text{C}(\text{CF}_3\text{SO}_2)_3]^-$ , and TFSM,  $[\text{CH}(\text{CF}_3\text{SO}_2)_2]^-$ . The calculated structure of the TriTFSM anion was recently reported by Zhang et al.,<sup>3</sup> using the same level of calculation as the present work uses. Experimentally this anion has been obtained only with large synthesis efforts and sometimes with unambiguous identification.<sup>5–7</sup> Turowsky et al. reported the crystal structure of the monohydrate potassium salt.<sup>5</sup> The extra ligand on the central C atom, compared to the nitrogen-based TFSI anion, can for both anions intuitively be expected to provide a more extensively delocalized charge.

The TFSM anion has been reported to be unstable vs reduction<sup>8</sup> and is therefore not likely to be a high-voltage-battery electrolyte component, but the structural information and the

comparison with the trisubstituted TriTFSM anion may nevertheless provide important information on further synthesis possibilities.

By calculating the lithium ion interaction energies, the anions' possibilities as SPE salt candidates can be assessed from an ion–ion dissociation point of view. Gejji et al. have calculated several stable structures, vibrational frequencies, and the interaction energies of Li–TFSI ion pairs.<sup>9</sup> In the present work the calculated IR and Raman spectra for the two anions and their ion pairs with lithium are reported to provide a basis for fingerprinting the different species experimentally. These spectra can also be compared with the calculated spectra for TFSI<sup>4</sup> and PFSI.<sup>2</sup> Apart from the characterization IR spectra from the original salt synthesis papers, Aurbach et al.<sup>10</sup> have measured the spectra of the TriTFSM anion both in situ and ex situ using different surface IR techniques. Those spectra provide realistic guidelines for the difficulties of species identification, and show where the present calculations can be of assistance. Tentative assignments for some vibrational bands are made on the basis of visual analysis of the modes and earlier work.

The calculations were performed on the  $[\text{C}(\text{CF}_3\text{SO}_2)_3]^-$  and  $[\text{CH}(\text{CF}_3\text{SO}_2)_2]^-$  anions as well as the  $\text{Li}^+[\text{C}(\text{CF}_3\text{SO}_2)_3]^-$  and  $\text{Li}^+[\text{CH}(\text{CF}_3\text{SO}_2)_2]^-$  ion pairs using semiempirical, ab initio Hartree–Fock (HF) and density functional theory (DFT) methods.

## Calculational Method

Semiempirical PM3 methods were used to locate the preferred positions for lithium ion coordination as well as to provide starting geometries for the higher level anion calculations. The lithium ion starting positions were initially chosen to be several different positions adjacent to the negative centra of the anions.

Subsequently ion pairs and anion conformers were treated with ab initio self-consistent field molecular orbital (SCF-MO) HF methods (HF/6-31G\*). This calculational level has previously been shown to provide both structures and spectra with reasonable accuracy for the TFSI and PFSI anions<sup>1,2,4</sup> and is generally considered cost-effective for producing vibrational spectra.<sup>11</sup> Only the most stable anion conformer and ion pair for each choice of anion are reported. To obtain the binding energies, single-point calculations were performed, without any

<sup>†</sup> E-mail: patrikj@fy.chalmers.se.

BSSE correction. Two binding energies are calculated and defined as  $E_{\text{bind}} = E_{\text{ion pair}} - E_{\text{anion in ion pair geometry}} + E_{\text{Li}^+}$  and  $E_{\text{bind2}} = E_{\text{ion pair}} - (E_{\text{anion-free}} + E_{\text{Li}^+})$ .

Analytical second derivatives were calculated to confirm the minima and to produce the vibrational spectra. Only vibrational frequencies that have IR intensities stronger than 5.0 km mol<sup>-1</sup> or Raman activities stronger than 1.0 Å<sup>4</sup> amu<sup>-1</sup> are reported. The recommended scaling factors for HF/6-31G\* general frequencies and low-frequency vibrations are 0.8953 and 0.9061,<sup>11</sup> respectively, and therefore a scaling factor of 0.90 was generally applied.

DFT calculations (B3LYP/6-31G\*) were performed, using the obtained HF structures as starting values, to include and evaluate the effects of electron correlation, which is treated in the hybrid B3LYP exchange functional.<sup>12,13</sup> The B3LYP functional was chosen on the basis of its reported accurate performance with the 6-31G\* basis set at a reasonable computational cost.<sup>11,14</sup> Here, the vibrational spectra were again calculated, but Raman activities were excluded for CPU time savings as they are not yet available by analytical methods and numerical methods would involve a large additional CPU cost. No frequency scaling was performed due to the differing scaling factors for general frequencies and low-frequency vibrations of 0.9614 and 1.0013, respectively.<sup>11</sup>

Additional single-point calculations (HF/6-311+G\*\*//HF/6-31G\*) were performed to obtain more accurate values for the HOMO and LUMO for the two anions.

All calculations were performed using the Gaussian98 program suite (revision A.7).<sup>15</sup>

## Results and Discussion

The prime interest is the obtained differences between the two anions and a comparison with previous experimental and calculational work. Second, the ion pairs' differences and characteristics are summarized, with special attention paid to the possibilities for experimental species detection.

**[C(CF<sub>3</sub>SO<sub>2</sub>)<sub>3</sub>]<sup>-</sup> and [CH(CF<sub>3</sub>SO<sub>2</sub>)<sub>2</sub>]<sup>-</sup> Anions. Geometry and Charge Distribution.** The obtained energy minimum structures (B3LYP/6-31G\*) are depicted in Figure 1. Selected geometry parameters and energies are reported in Table 1. As expected most of the B3LYP calculated values for TriTFSM are identical to those reported in ref 3. The two anions are structurally similar in many aspects, but here a summary of the most important differences and how they compare with existing experimental data is made. As mentioned in the Introduction, the crystal structure of K<sup>+</sup>-[C(CF<sub>3</sub>SO<sub>2</sub>)<sub>3</sub>]<sup>-</sup>·H<sub>2</sub>O has been determined<sup>5</sup> and will serve as an experimental comparison for TriTFSM, while for TFMSM no suitable experimental structure determination has been found.

First of all, though, a comment on HF vs B3LYP calculations: as expected the bond lengths increase (by 0.2–0.6 Å) when electron correlation is included, while most angles are remarkably unchanged. From a structural point of view, the use of B3LYP does not seem critical to provide at least *qualitatively* correct structures, but this might change for the noncovalent interactions present in the ion pairs. In fact, for TriTFSM the HF bond distances S<sub>x</sub>-C1, S-O, S-C<sub>x</sub>, and C-F<sub>x</sub> are in generally better agreement than the B3LYP values with the crystal structure—within 0.3 Å of the average experimental bond distances. However, this might be due to the K<sup>+</sup> cation coordination induced changes to the anion in the experimental study. If this is true, B3LYP may perform better than HF in a comparison based on the TriTFSM ion pair. Unfortunately, data that could partly prove/dismiss a deficiency in the methods, a

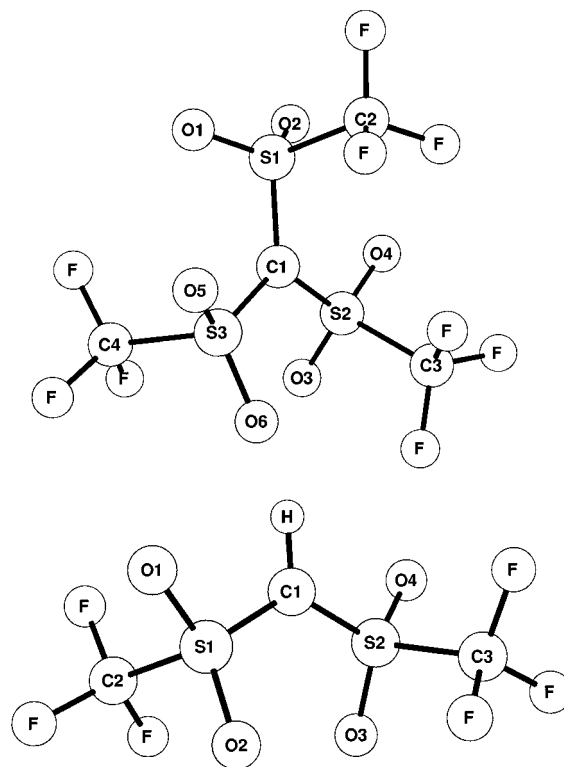


**Figure 1.** Minimum-energy structure of the (a, top) TriTFSM anion and (b, bottom) TFMSM anion.

crystal structure with the cation outside the first coordination sphere of the anion, as for TFSI in ref 16, cannot be found for TriTFSM.

Experimentally the three central S-C-S angles are on average 121.6°, while (on average) 120.0° in the HF calculations. Also the O-S-O and the C-S-C angles (120.1° and 105.7°) are well reproduced in the calculations (119.7° and 106.5°). In light of a comparison with a crystal structure, where the anion entity is directly coordinated by a cation, and where the estimated standard deviations are 0.003–0.008 Å and 0.2–0.5°, the calculation also gives a *quantitative* representation of the anion structure even at the HF level. Also the asymmetry of the CF<sub>3</sub>SO<sub>2</sub> groups with respect to the CS<sub>3</sub> plane, as in the crystal, can be observed in Figure 1a.

The TFMSM anion can now be compared with the TFSI and the TriTFSM anions, as well as with earlier calculations on TFMSM.<sup>17,18</sup> The most significant changes will most likely originate in the protonation at the central carbon atom and the significantly more open structure compared to that of TriTFSM. The TFMSM anion has striking similarities with the TFSI anion: a S-C-S (S-N-S) central angle of ~127° (127°) and two S-C-S-C dihedral angles of ~87° (~93°). Thus, the TFMSM anion has approximate C<sub>2</sub> symmetry, as does the most stable TFSI conformer, even if no such restriction was applied in the geometry optimizations. This is in contrast to the C<sub>1</sub> symmetry TriTFSM anion. A larger internal flexibility for the TFMSM anion compared to the TriTFSM anion can be expected due to more space available for conformational changes. The central unit in TFMSM (CS<sub>2</sub>H) keeps the planar arrangement found for TriTFSM (CS<sub>3</sub>). The values reported in refs 17 and 18 are about the same, even though a smaller basis set (3-21+G\*) was used. The main difference is that the C-F distances are better reproduced in the present paper (exptl ~1.32 Å,<sup>17,18</sup> 1.37 Å).

Furthermore, like the TFSI anion, TFMSM has a large double bond character for the central S<sub>x</sub>-C1 (S-N) bonds. The central

**TABLE 1: Selected Geometry Parameters for the Anion Bond Lengths ( $r$ ) (Å) and Bond Angles ( $a, d$ ) (deg)**

	[C(CF <sub>3</sub> SO <sub>2</sub> ) <sub>3</sub> ] <sup>-</sup>		[CH(CF <sub>3</sub> SO <sub>2</sub> ) <sub>2</sub> ] <sup>-</sup>	
	HF	B3LYP	HF	B3LYP
$r(\text{C}_x\text{-F}_x)$ (av CF <sub>3</sub> )	1.311	1.339	1.317	1.344
$r(\text{S1-C2})$	1.825	1.879	1.824	1.877
$r(\text{S2-C3})$	1.853	1.908	1.824	1.877
$r(\text{S3-C4})$	1.827	1.880		
$r(\text{S1-O1})$	1.428	1.466	1.439	1.477
$r(\text{S1-O2})$	1.425	1.463	1.434	1.471
$r(\text{S2-O3})$	1.428	1.466	1.434	1.471
$r(\text{S2-O4})$	1.428	1.465	1.439	1.477
$r(\text{S3-O5})$	1.426	1.464		
$r(\text{S3-O6})$	1.432	1.469		
$r(\text{S1-C1})$	1.725	1.745	1.670	1.690
$r(\text{S2-C1})$	1.735	1.755	1.670	1.690
$r(\text{S3-C1})$	1.719	1.741		
$r(\text{C1-H})$			1.069	1.080
$a(\text{O1-S1-O2})$	119.4	119.9	120.0	120.6
$a(\text{O3-S2-O4})$	120.0	120.3	120.0	120.6
$a(\text{O5-S3-O6})$	119.8	120.0		
$a(\text{O1-S1-C1})$	108.9	109.4	108.9	108.8
$a(\text{O2-S1-C1})$	112.9	112.5	114.1	114.0
$a(\text{O3-S2-C1})$	112.5	112.1	114.1	114.0
$a(\text{O4-S2-C1})$	108.6	109.6	108.9	108.8
$a(\text{O5-S3-C1})$	113.2	112.9		
$a(\text{O6-S3-C1})$	107.3	108.3		
$a(\text{C2-S1-C1})$	105.4	104.7	107.1	106.8
$a(\text{C3-S2-C1})$	107.0	105.7	107.1	106.8
$a(\text{C4-S3-C1})$	107.1	105.7		
$a(\text{S1-C1-S2})$	121.4	121.7	127.5	126.9
$a(\text{S1-C1-S3})$	120.3	120.1		
$a(\text{S2-C1-S3})$	118.3	118.0		
$d(\text{S1-C1-S2-C3})$	114.3	110.1	-87.7	-86.5
$d(\text{S1-C1-S3-C4})$	84.7	87.0		
$d(\text{S2-C1-S1-C2})$	-83.8	-83.7	-87.7	-86.5
$d(\text{S2-C1-S3-C4})$	-96.1	-96.6		
$d(\text{S3-C1-S1-C2})$	95.4	92.5		
$d(\text{S3-C1-S2-C3})$	-64.9	-66.2		
$d(\text{H-C1-S1-C2})$			92.4	93.6
$d(\text{H-C1-S2-C3})$			92.2	93.4
$E$ (au)	-2687.910889	-2696.726915	-1805.162758	-1811.139599

**TABLE 2: Mulliken Charges for the Anions (HF/6-31G\*)**

atom	[C(CF <sub>3</sub> SO <sub>2</sub> ) <sub>3</sub> ] <sup>-</sup>	[CH(CF <sub>3</sub> SO <sub>2</sub> ) <sub>2</sub> ] <sup>-</sup>	atom	[C(CF <sub>3</sub> SO <sub>2</sub> ) <sub>3</sub> ] <sup>-</sup>	[CH(CF <sub>3</sub> SO <sub>2</sub> ) <sub>2</sub> ] <sup>-</sup>
H		0.26	O4	-0.68	-0.70
C1	-1.13	-0.98	O5	-0.65	
S1	1.54	1.46	O6	-0.67	
S2	1.52	1.46	C2	0.85	0.83
S3	1.54		C3	0.84	0.83
O1	-0.66	-0.70	C4	0.84	
O2	-0.66	-0.69	F <sub>x</sub> (av CF <sub>3</sub> )	0.33	0.35
O3	-0.70	-0.69			

S<sub>x</sub>-C1 bonds are shorter than the “outer” S<sub>x</sub>-C(x + 1) bonds by 0.154 Å at the HF level and 0.187 Å at the B3LYP level. The S<sub>x</sub>-C1 double bond character is less pronounced for TriTFSM, the “outer” S-C lengths are about the same as for TFMSM, and thus the differences are smaller (0.109 and 0.142 Å). The reason seems to be the electron density donated from the hydrogen in TFMSM, which then is delocalized onto the central S<sub>x</sub>-C1 bonds, while no such donating group exists for TriTFSM. Other changes for TFMSM compared to TriTFSM are mainly found for the S-O bond lengths, which are slightly longer than in TriTFSM.

In Table 2 the Mulliken charges (HF) for the two anions are listed. The charges support the above reasoning: the hydrogen has a low positive charge, the negative charge on C1 (TFMSM) is readily reduced compared to that on C1 (TriTFSM), and the TFMSM sulfurs are slightly less positive than those in TriTFSM.

In two previous studies, employing the HF/3-21+G\* calcu-

lational level, the free triflate, TFSI, and TFMSM anions<sup>17</sup> as well as their ion pairs with lithium were investigated.<sup>18</sup> On the basis of the HSAB principle and the chemical hardness, the TFMSM anion was shown to have a lower lithium affinity than triflate and TFSI. The TFMSM anion results, geometry and charge distribution, are in agreement with those of the present work; no large differences in geometry are observed compared to the present HF/6-31G\* or B3LYP/6-31G\* levels of calculation. But, on the other hand, the values for TFSI in ref 17 might be questioned as they report a S-N-S angle of 156°, which clearly is far too large.<sup>1,4</sup> Therefore, the affinity comparison might not be valid.

In ref 2 a chemical hardness ( $\eta$ ) scale was presented for several anions used in SPEs including TFSI and PFSI. The hardness value was calculated as half the difference between the HOMO and LUMO using the values from HF/6-311+G\*\*//HF/6-31G\* calculations. Using this methodology, the TFMSM and TriTFSM show values of 5.74 and 6.32 eV, respectively. The hardness value combined with the high HOMO level for TFMSM (-6.65 eV) corresponds well to the electrochemical instability reported earlier.<sup>8</sup> Also TriTFSM seems less hard and less stable than do TFSI or PFSI, but only marginally.

*Vibrational Spectra.* In Tables 3 and 4 selected calculated frequencies, IR intensities, and Raman activities are tabulated for the free anions. The analysis starts with a general comparison between the methods chosen and continues with the calculated

**TABLE 3: Selected Vibrational Frequencies, Infrared Intensities, and Raman Activities for the [C(CF<sub>3</sub>SO<sub>2</sub>)<sub>3</sub>]<sup>-</sup>Anion**

HF				B3LYP	
$\nu$ (unscaled) (cm <sup>-1</sup> )	$\nu$ (scaled) ( $\times 0.90$ )	IR intens (km mol <sup>-1</sup> )	Raman activity (A <sup>4</sup> amu <sup>-1</sup> )	$\nu$ (unscaled) (cm <sup>-1</sup> )	IR intens (km mol <sup>-1</sup> )
251	226				
280	252		3.1		
284	256		3.2		
304	274		1.9		
310	279		3.3		
328	295		2.6		
347	312		2.7		
367	330		1.6		
379	341		4.4		
414	373		1.9		
424	382	12	1.5	370	7
435	392	11			
478	430			405	15
568	511			502	68
570	513	68		503	60
585	527		1.3		
606	545		2.0		
607	546		1.4		
632	569	21		553	12
635	572		1.6		
643	579	112	3.3	565	74
656	590	168	1.3	570	121
726	653	450		624	351
764	688	49	3.0	673	
857	771	28			
860	774	13	10.6		
1090	981	202		942	206
1112	1001	218		963	227
1236	1112	139	3.0	1099	87
1241	1117	179	6.2	1102	
1250	1125	287	12.9	1111	
1361	1225	189	4.6	1182	107
1378	1240	230	1.2	1195	270
1381	1243	330	2.0	1213	
1390	1251	196	2.9	1215	
1394	1255	276	1.1	1224	159
1402	1262	248	3.3	1229	190
1405	1265	86	4.7	1239	236
1413	1272	151		1247	161
1421	1279	40	1.7	1255	66
1453	1308	26	2.4	1307	13
1492	1343	568	3.2	1339	347
1495	1346	551	3.2	1343	

spectra of the two anions. All frequencies are scaled HF values unless explicitly stated otherwise.

In general the obtained frequencies from the B3LYP calculations (unscaled) are *lower* than those from HF (scaled), which perhaps is surprising. This is probably due both to the exaggerated bond strengths in the HF calculations and to a basis set not flexible enough. For the higher frequencies the difference is negligible. By using also the IR intensities, however, the corresponding bands from the two methods are easily matched to one another throughout the entire spectral range. Going from HF to B3LYP, the IR intensities are reduced by as much as 50% for some bands. However, we have no means to determine which method gives the more correct values, even if the B3LYP method is believed to give better accuracy.<sup>14</sup>

The most striking difference between the two calculated anion spectra, apart from the obvious C–H stretching band at  $\sim 3100$  cm<sup>-1</sup>, is the triplet of bands at 1308, 1343, and 1346 cm<sup>-1</sup> in TriTFSM, which only has a doublet counterpart in TFSM (1309 and 1315 cm<sup>-1</sup>). This can be expected from the molecular structure, but what is surprising is the drastically lower IR intensity for the 1308 cm<sup>-1</sup> band compared to all the others. A similar doublet was found for TFSI, and was found to originate in the possibility of two different  $\nu_{as}(\text{SO}_2)$  stretchings, with the

**TABLE 4: Selected Vibrational Frequencies, Infrared Intensities, and Raman Activities for the [CH(CF<sub>3</sub>SO<sub>2</sub>)<sub>2</sub>]<sup>-</sup>Anion**

HF				B3LYP	
$\nu$ (unscaled) (cm <sup>-1</sup> )	$\nu$ (scaled) ( $\times 0.90$ )	IR intens (km mol <sup>-1</sup> )	Raman activity (A <sup>4</sup> amu <sup>-1</sup> )	$\nu$ (unscaled) (cm <sup>-1</sup> )	IR intens (km mol <sup>-1</sup> )
				208	9.3
287	258		1.1		
298	268		5.0		
340	306		3.3		
371	334		3.9		
391	352	10		331	9
421	379		1.6	369	6
425	383		1.9		
519	467	45	2.1	454	50
556	500	92		490	65
576	518		1.1		
604	544		1.3		
607	546		1.8		
626	563	58	3.6	555	35
637	573		2.1		
691	622	526		596	375
702	632	11		618	8
837	753		14.4		
844	760	28		746	5
922	830	36	3.9	833	27
1070	963	392		966	395
1208	1087	386	1.3	1086	285
1235	1112		13.6		
1361	1225	129	1.5	1195	238
1367	1230	219	1.1	1201	286
1382	1244	14	1.1	1202	202
1383	1245	525	1.5		
1392	1253	7	1.6	1227	71
1403	1263	249	2.5	1227	56
1405	1265	8	8.4	1238	256
1454	1309	239		1307	119
1461	1315	709	1.4	1315	438
3449	3104	6	65.1		

two SO<sub>2</sub> groups vibrating in-phase or out-of-phase. For TFSM the split between the two is smaller (6 cm<sup>-1</sup>) than for TFSI (25 cm<sup>-1</sup>), but the IR intensity ratios are similarly sized (4.6 and 3.0, respectively). On the other hand, for TriTFSM, the split is larger and about the same as for TFSI ( $\sim 27$  cm<sup>-1</sup>), but the intensity ratios are as large as  $\sim 20$ . The origin of the triplet, found by visualizing the modes, is that the two higher modes are different in-phase  $\nu_{as}(\text{SO}_2)$  combinations, but the lower mode is a completely out-of-phase  $\nu_{as}(\text{SO}_2)$  combination. The lower symmetry of the TriTFSM anion leads to even lower intensity for this band than for TFSM and TFSI.

The many bands at  $\sim 1220$ – $1280$  cm<sup>-1</sup> all originate from different C–F stretchings, and even if they are strong bands and probably can be detected in any measurement, they overlap and make any detailed analysis difficult.

The bands at 1087 and 1112 cm<sup>-1</sup> for TFSM are the corresponding two  $\nu_s(\text{SO}_2)$  bands, the higher frequency being in-phase (among the highest Raman activities); for the lower frequency, the hydrogen also contributes to the mode and has a high IR intensity. As was found for the  $\nu_{as}(\text{SO}_2)$  bands, the TriTFSM spectra have a triplet instead of a doublet (1112, 1117, and 1125 cm<sup>-1</sup>).

Next in the spectra are the bands at 963 cm<sup>-1</sup> (TFSM) and 981 and 1001 cm<sup>-1</sup> (TriTFSM). The TFSM band is mainly  $\nu_{as}(\text{C–S})$ , but also the hydrogen moves in the CS<sub>2</sub> plane stiffly on the C–H axis. For TriTFSM the band doublet corresponds to two different movements of the carbon atom in the CS<sub>3</sub> plane to positions between two sulfurs from CF<sub>3</sub>SO<sub>2</sub> groups pointing in opposite directions. Only two such movements are possible for structural reasons, and therefore there is no triplet. The



**TABLE 5: Selected Geometry Parameters for the Ion Pair Bond Lengths ( $r$ ) (Å) and Bond Angles ( $a, d$ ) (deg)**

	$\text{Li}^+ - [\text{C}(\text{CF}_3\text{SO}_2)_3]^-$		$\text{Li}^+ - [\text{CH}(\text{CF}_3\text{SO}_2)_2]^-$	
	HF	B3LYP	HF	B3LYP <sup>a</sup>
$r(\text{C}_x - \text{F}_x)$ (av $\text{CF}_3$ )	1.305	1.331	1.311	1.337
$r(\text{S1} - \text{C2})$	1.856	1.914	1.823	1.879
$r(\text{S2} - \text{C3})$	1.828	1.884	1.823	1.879
$r(\text{S3} - \text{C4})$	1.828	1.883		
$r(\text{S1} - \text{O1})$	1.419	1.456	1.424	1.46
$r(\text{S1} - \text{O2})$	1.460	1.500	1.465	1.505
$r(\text{S2} - \text{O3})$	1.458	1.499	1.465	1.505
$r(\text{S2} - \text{O4})$	1.417	1.454	1.424	1.46
$r(\text{S3} - \text{O5})$	1.428	1.465		
$r(\text{S3} - \text{O6})$	1.421	1.459		
$r(\text{S1} - \text{C1})$	1.727	1.745	1.667	1.687
$r(\text{S2} - \text{C1})$	1.714	1.729	1.667	1.687
$r(\text{S3} - \text{C1})$	1.740	1.773		
$r(\text{C1} - \text{H})$			1.071	1.082
$r(\text{Li} - \text{O2})$	1.818	1.797	1.832	1.823
$r(\text{Li} - \text{O3})$	1.823	1.803	1.831	1.823
$a(\text{O1} - \text{S1} - \text{O2})$	117.3	117.4	118.8	119.3
$a(\text{O3} - \text{S2} - \text{O4})$	117.5	117.2	118.8	119.3
$a(\text{O5} - \text{S3} - \text{O6})$	121.5	121.6		
$a(\text{O1} - \text{S1} - \text{C1})$	113.6	113.5	112.2	111.8
$a(\text{O2} - \text{S1} - \text{C1})$	107.5	108.6	111.3	111.2
$a(\text{O3} - \text{S2} - \text{C1})$	111.2	111.4	111.3	111.1
$a(\text{O4} - \text{S2} - \text{C1})$	111.0	111.3	112.2	111.8
$a(\text{O5} - \text{S3} - \text{C1})$	105.7	106.2		
$a(\text{O6} - \text{S3} - \text{C1})$	111.2	111.1		
$a(\text{C2} - \text{S1} - \text{C1})$	109.1	108.2	107.6	108.3
$a(\text{C3} - \text{S2} - \text{C1})$	107.6	107.4	107.6	108.4
$a(\text{C4} - \text{S3} - \text{C1})$	106.3	104.5		
$a(\text{S1} - \text{C1} - \text{S2})$	123.9	124.7	127.2	126.5
$a(\text{S1} - \text{C1} - \text{S3})$	116.7	116.0		
$a(\text{S2} - \text{C1} - \text{S3})$	119.3	118.7		
$d(\text{S1} - \text{C1} - \text{S2} - \text{C3})$	83.2	79.5	-93.5	-88.0
$d(\text{S1} - \text{C1} - \text{S3} - \text{C4})$	96.2	98.2		
$d(\text{S2} - \text{C1} - \text{S1} - \text{C2})$	-108.4	-104.5	-93.6	-88.1
$d(\text{S2} - \text{C1} - \text{S3} - \text{C4})$	-88.5	-89.8		
$d(\text{S3} - \text{C1} - \text{S1} - \text{C2})$	66.6	66.9		
$d(\text{S3} - \text{C1} - \text{S2} - \text{C3})$	-91.6	-91.7		
$d(\text{H} - \text{C1} - \text{S1} - \text{C2})$			86.4	92.1
$d(\text{H} - \text{C1} - \text{S2} - \text{C3})$			86.4	91.8
$E$ (au)	-2695.364339	-2704.241274	-1812.633258	-1818.672918
$E_{\text{w/o Li}^+}$ (au)	-2687.902464	-2696.718511	-1805.153082	-1811.130720
$E_{\text{bind}}$ (kJ mol <sup>-1</sup> ) <sup>b</sup>	594	625	642	677
$E_{\text{bind2}}$ (kJ mol <sup>-1</sup> ) <sup>b</sup>	572	603	617	653

<sup>a</sup> One low imaginary frequency. <sup>b</sup>  $E_{\text{Li}^+} = -7.235536$  and  $-7.284544$  au, respectively.

inherent low symmetry in these vibrations also explains their negligible Raman activity.

For TriTFSM there is then a  $\sim 200$  cm<sup>-1</sup> wide empty space in the spectrum, and for TFSM as well, apart from a band at 830 cm<sup>-1</sup>, which clearly does not have a direct TriTFSM counterpart. This is a  $\nu_s(\text{C}-\text{S})$  band, which explains the high Raman activity. Thus, this is the best candidate for experimental discrimination of the two anions: high Raman intensity and is probably also visible in the IR spectra, no counterpart in TFSM, and no other bands interfering.

Next consider the region 600–800 cm<sup>-1</sup>; this is the region for TFSI where bands are found which can be used for detection of ion pairs,<sup>4,9</sup> but also a region where coupling between different internal coordinates can make modes easily move in the spectra relative to one another. Judging from the Raman activities, the bands at 753 (TFSM) and 774 (TriTFSM) cm<sup>-1</sup> seem to be corresponding. These are both modes due to an expansion/contraction of the whole anion. This type of mode was also observed for TFSI and assigned as mainly a  $\nu_s(\text{S}-\text{N}-\text{S})$  mode,<sup>4</sup> and should thus accordingly be tentatively assigned as  $\nu_s(\text{S}-\text{C}-\text{S})$ . Any such classification is however an

oversimplification of this complex mode type. The 760 cm<sup>-1</sup> band for TFSM corresponds to the 771 cm<sup>-1</sup> band for TriTFSM, and they are both  $\nu(\text{C}-\text{F})$  and  $\nu(\text{C}-\text{S})$  coupled modes. The next doublet, for both TFSM and TriTFSM, has one very intense IR band, C–S–C bending out-of-plane, and one less intense IR band, almost pure in-plane C–S–C bending (TFSM) and  $\nu_s(\text{C}-\text{S})$  (TriTFSM). The latter is thus the TriTFSM band corresponding to the 830 cm<sup>-1</sup> TFSM band, and there is no possibility for a single in-plane  $\delta(\text{C}-\text{S}-\text{C})$  band for TriTFSM.

Below 600 cm<sup>-1</sup> there are many modes close in energy, and any attempt of assignment will be affected by coupling between the various modes. Also, for SPE purposes, this region has many bands arising from the PEO polymer, and therefore no attempt to assign these bands is made.

Having made a calculational assignment, comparisons with the existing and relevant experimental data are easier. For TriTFSM the work by Aurbach et al.<sup>10</sup> provides data which possibly can be interpreted as being for a “free” anion in a solvent/polymer matrix—excellent realistic data sets for our purposes. For TFSM, however, the IR data from the original lithium salt synthesis<sup>19</sup> are the choice of comparison, as no other

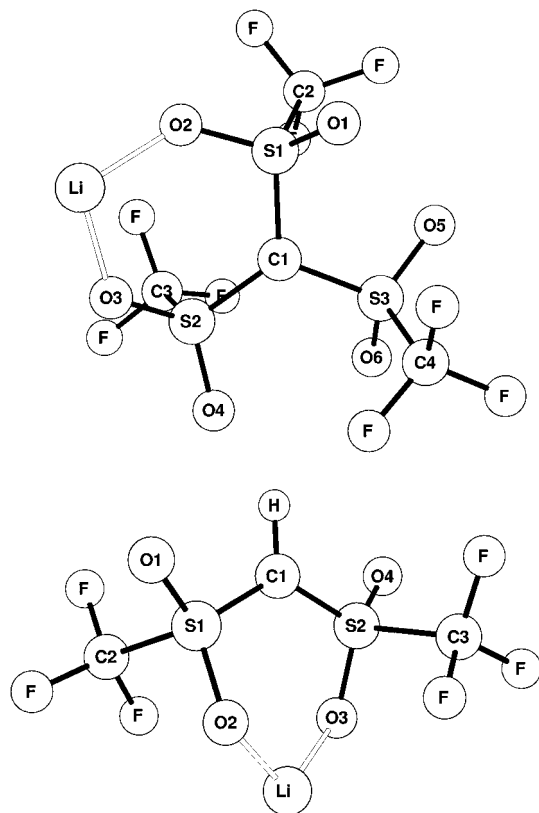


**Figure 2.** Minimum-energy structure of the (a, top) Li–TriTFSM ion pair and (b, bottom) Li–TFSM ion pair.

experimental data exist. Similarly for TriTFSM the cesium salt IR data are the choice of comparison.<sup>5</sup>

In total, 13 bands are reported for LiTFSM, and the calculated values are on average  $\sim 20$   $\text{cm}^{-1}$  from those values (absolute deviation): 3083 m (21), 1341 vs (26), 1316 vs (7), 1241 w (22), 1227 m (18), 1198 vs (32), 1134 m (22), 1093 m (6), 983 m (20), 846 w (16), 659 w (27), 587 m (35), and 503 w (3)  $\text{cm}^{-1}$ . Only within the C–F stretching region (1100–1300  $\text{cm}^{-1}$ ), where many bands overlap, is the exact correspondence unclear. Also, the original spectrum is not given in ref 19, and a totally justified comparison is therefore not possible. The IR intensities have worse correspondence, an effect of both the calculational level and the nature of the comparison.

On the other hand, for TriTFSM, two comparisons can be made. Comparing first with the work of Aurbach et al. using many different surface IR techniques (SNIFTIRS, SIR, ATR) in different solvents (THF, 1,3-dioxolane), the following relevant peak regions from the samples are observed: 1365–1380, 1207–1245, 1150–1175, 1100–1130, 1060–1080, 1020–1050, 956–980, and 900  $\text{cm}^{-1}$ . The calculated  $\nu_{\text{as}}(\text{SO}_2)$  values are thus  $\sim 30$   $\text{cm}^{-1}$  too low (as for the highest TFSM component), and the C–F stretching region is similarly difficult to analyze. The region 1100–1130  $\text{cm}^{-1}$  corresponds nicely to the band triplet at 1112, 1117, and 1125  $\text{cm}^{-1}$ , easily identified by empty regions of  $\sim 100$   $\text{cm}^{-1}$  on both sides. Here possibly also the observed 1060–1080  $\text{cm}^{-1}$  bands should be included. The 1020–1050  $\text{cm}^{-1}$  bands are assigned<sup>10</sup> to  $\nu(\text{S–O})$ , single-bonded, which should not be present in this anion. However, in the experiment also different electrochemical decomposition products are probed. The 956–980  $\text{cm}^{-1}$  bands are easily fitted against our calculated 981  $\text{cm}^{-1}$  band and thus assigned as a C–S bending mode, and not as  $\delta(\text{S–O})$ .<sup>10</sup> Finally the 900  $\text{cm}^{-1}$  band obviously has no correspondence in the calculations, and thus should be due to solvent or decomposition products.

In the second comparison the IR data for CsTriTFSM (KBr pellet) from ref 5 are used. The  $\text{Cs}^+$  cation should have a negligible effect on the anion, but clearly crystal packing may occur. Proceeding as for LiTFSM, 19 bands are reported: 2923 w and 2853 w (both probably due to residual solvent), 1385 s (39), 1373 vs (30), 1334 m (26), 1230 s (13), 1196 vs (29), 1131 s (6), 1121 s (4), 970 s (11), 776 w (2), 765 w (6), 693 s (40), 609 s (19), 584 s (5), 515 s (2), 427 w (3), 393 w (1), and 279 w (0)  $\text{cm}^{-1}$ . The C–F region is also here ambiguous, but the current assignment renders the average deviation  $\sim 14$   $\text{cm}^{-1}$ . The only other difficulty is the 693  $\text{cm}^{-1}$  band, for which two calculated candidates exist: 653 and 688  $\text{cm}^{-1}$ . The former was chosen due to the much stronger calculated IR intensity ( $\sim 9$  times stronger). All other bands fit extremely well, especially when taking the nature of comparison into account.

To summarize, for both anions the calculations show experimental agreement within  $\sim 20$   $\text{cm}^{-1}$ , even when the more difficult C–F regions are included. For bands below 1100  $\text{cm}^{-1}$  the deviation is  $\sim 18$  and  $\sim 9$   $\text{cm}^{-1}$ , respectively. The stronger effect on the anion imposed by  $\text{Li}^+$  rather than  $\text{Cs}^+$  is a likely cause of the worse agreement for TFSM compared to TriTFSM.

**Li[C(CF<sub>3</sub>SO<sub>2</sub>)<sub>3</sub>] and Li[CH(CF<sub>3</sub>SO<sub>2</sub>)<sub>2</sub>] Ion Pairs. Geometry and Binding Energies.** From the previous section some differences in the two anions' complexation of a lithium ion can be expected. In Figure 2 the most stable ion pairs with lithium obtained (B3LYP/6-31G\*) for each choice of anion are depicted, and the resulting energies and selected geometry parameters are reported in Table 5. Using any of the calculated binding energies, the lithium cation binds to the TFSM anion  $\sim 50$   $\text{kJ mol}^{-1}$  stronger than it binds to the TriTFSM anion. The TriTFSM  $E_{\text{bind}}$  value is in fact  $\sim 35$   $\text{kJ mol}^{-1}$  lower than for TFSI,<sup>9</sup> suggesting it to be a suitable SPE salt anion candidate. Furthermore, due to the bulky anion, another beneficial factor in real SPE systems—a lower contribution of anion conductivity to the total ion conductivity—can be expected. However, it is still unclear whether a plasticizing effect similar to that obtained with TFSI can be attributed TriTFSM.

The cation interaction is for both anions bidentate to oxygen atoms from two different  $\text{SO}_2$  groups. An inverse proportionality of Li–O bond lengths and binding energy can be observed: at the HF level the Li–O bonds in Li–TFSM are  $\sim 0.011$  Å longer than in Li–TriTFSM. This value is doubled using DFT methods ( $\sim 0.023$  Å). However, the S–O<sub>Li-bonded</sub> bonds are within  $\sim 0.007$  Å of each other at each computational level, and the induced changes in the S–O bonds upon lithium coordination are  $\sim 0.03$  Å regardless of both the anion and the level of calculation.

Compared to the previous calculation on Li–TFSM (conformer b3<sup>18</sup>), our geometry differs in only a few aspects: the C–F distances are shorter, the central C1–S<sub>x</sub> bonds longer, and the S–O bonds are somewhat shorter. However, the induced changes upon cation coordination are on par. In ref 18 the S–O bond length differences between the isolated anion and the “b3” ion pair are  $+0.29$  Å (Li-coordinated) and  $-0.16$  Å (uncoordinated). Our values are  $+0.31$  and  $-0.15$  Å, respectively. Totally, the TFSM anion entity is not severely affected by the cation—at least not structurally.

For Li–TriTFSM no previous calculation exists. Compared to the anion, the most pronounced changes are the elongated S–O bonds due to cation coordination. Comparison with the crystal structure of  $\text{K}^+[\text{C}(\text{CF}_3\text{SO}_2)_3]^- \cdot \text{H}_2\text{O}^5$  shows correspondence similar to that for the pure anion. No crystal structure determination with the more interacting lithium cation exists.

**Vibrational Spectra.** To assist eventual detection of ion pairs in experimental spectra, an analysis is made on the induced

changes compared to the pure anion spectra. Ideally no ion pairs should be present in the SPEs at the working temperature. Apart from a significantly sized shift, the bands, from both the “free” anions and the ion pairs, should easily be detected by either IR or Raman spectroscopy. In the anion section an analysis was made upon which this analysis must start: the C–F region and the bands below  $600\text{ cm}^{-1}$  are seemingly not good candidates, while the bands below  $1200\text{ cm}^{-1}$  seem to provide opportunities. For TFMS the lithium cation coordination causes the two  $\nu_s$ -( $\text{SO}_2$ ) bands ( $1112$  and  $1087\text{ cm}^{-1}$ ) to shift by  $\sim 30\text{ cm}^{-1}$  ( $1086$  and  $1053\text{ cm}^{-1}$ ). It is clear from the IR and Raman intensities that the lower band is not fixed; for both the anion and ion pair, the higher frequency band in the doublet is a very strong Raman band, while the lower frequency band is strong in IR. If the salt is used in PEO, however, the  $\nu(\text{C–O–C})$  band of the polymer backbone occurs at about these frequencies, and therefore the current usage may be limited. The often used  $\sim 760\text{ cm}^{-1}$  (for TFSI) band is calculated to be  $753\text{ cm}^{-1}$  for the anion (strong in Raman), and for the ion pair the peak shifts to  $762\text{ cm}^{-1}$ . All bands in this region ( $600\text{--}1000\text{ cm}^{-1}$ ) shift only  $\sim 10\text{ cm}^{-1}$  due to cation coordination in the calculations. If possible to detect experimentally, a new band with no counterpart in the anion arises at  $\sim 433\text{ cm}^{-1}$ . The mode is almost entirely due to a moving lithium ion, and has  $\sim 30\text{ cm}^{-1}$  separation from all other bands. However, both the Raman and especially the IR intensities are low (7.4 and 1.2, respectively).

For TriTFMS the best candidates seem to be either the new bands arising at  $488$  and  $622\text{ cm}^{-1}$ , both strong in IR, or the shifted  $774\text{ cm}^{-1}$  anion band (to  $783\text{ cm}^{-1}$ , very strong in Raman).

### Concluding Remarks

The TriTFMS anion is probably a suitable SPE salt anion candidate: it has a low lithium affinity and low symmetry and is bulky. The electrochemical instability of TFMS has been confirmed. Using the present calculated IR and Raman spectra,

the two anions can be distinguished from one another, and the eventually occurring lithium ion pairs can easily be identified using different modes. The DFT calculated spectra provide no substantial enhancement on the spectrum quality in terms of comparison with the available experimental data.

**Acknowledgment.** This work was supported by a Senior Scientist Grant from the Nordic Energy Research Program (NERP).

### References and Notes

- (1) Johansson, P.; Gejji, S. P.; Tegenfeldt, J.; Lindgren, J. *Electrochim. Acta* **1998**, *43*, 1375.
- (2) Johansson, P.; Tegenfeldt, J.; Lindgren, J. *J. Phys. Chem. A* **2000**, *104*, 954.
- (3) Zhang, X.; Pugh, J. K.; Sukpirom, N.; Lerner, M. M. *Int. J. Inorg. Mater.* **2000**, *2*, 115.
- (4) Rey, I.; Johansson, P.; Lindgren, J.; Lassègues, J.-C.; Grondin, J.; Servant, L. *J. Phys. Chem. B* **1998**, *102*, 3249.
- (5) Turowsky, L.; Seppelt, K. *Inorg. Chem.* **1998**, *27*, 2135.
- (6) Gray, F. M. *Polymer Electrolytes*; RSC Materials Monographs; Royal Society of Chemistry: Cambridge, 1997; p 49.
- (7) Armand, M. *Solid State Ionics* **1996**, *89*, 5.
- (8) Benrabah, D.; Sanchez, J.-Y.; Armand, M. *Solid State Ionics* **1993**, *60*, 87.
- (9) Gejji, S. P.; Suresh, C. H.; Babu, K.; Gadre, S. R. *J. Phys. Chem. A* **1999**, *103*, 7474.
- (10) Aurbach, D.; Chusid, O.; Weissman, I.; Dan, P. *Electrochim. Acta* **1996**, *41*, 747.
- (11) Scott, A. P.; Radom, L. *J. Phys. Chem.* **1996**, *100*, 16502.
- (12) Becke, A. D. *J. Chem. Phys.* **1993**, *98*, 5648.
- (13) Lee, C.; Yang, W.; Parr, R. G. *Phys. Rev. B* **1988**, *37*, 785.
- (14) Wong, M. W. *Chem. Phys. Lett.* **1996**, *256*, 391.
- (15) Frisch, M. J.; et al. *GAUSSIAN 98*, Revision A.7; Gaussian Inc.: Pittsburgh, PA, 1995.
- (16) Haas, A.; Klare, Ch.; Betz, P.; Bruckmann, J.; Krüger, C.; Tsay, Y.-H.; Aubke, F. *Inorg. Chem.* **1996**, *35*, 1918.
- (17) Benrabah, D.; Arnaud, R.; Sanchez, J.-Y. *Electrochim. Acta* **1995**, *40*, 2437.
- (18) Arnaud, R.; Benrabah, D.; Sanchez, J.-Y. *J. Phys. Chem.* **1996**, *100*, 10882.
- (19) Holcomb, N. R.; Nixon, P. G.; Gard, G. L.; Nafshun, R. L.; Lerner, M. M. *J. Electrochem. Soc.* **1996**, *143*, 1297.